

EFFECT OF INCORPORATION OF BONE POWDER ON THE PHYSICAL PROPERTIES OF POLYPROPYLENE FUMARATE BASED BONE CEMENT

NAGWA A. KAMEL^{*,#}, SALWA L. ABD-EL-MESSIEH^{*}, SAMIA H. MANSOUR^{**},
K.N. ABD-EL-NOUR^{*}

^{*}Microwave Physics and Dielectrics Department, National Research Centre, Dokki, Cairo, Egypt,
[#]e-mail: nagwakamel@gmail.com

^{**}Polymers and Pigments Department, National Research Centre, Dokki, Cairo, Egypt

Abstract. Biodegradable and injectable composites based on polypropylene fumarate (PPF) as unsaturated polyester filled with 60 wt% of calcium sulphate dihydrate (gypsum) incorporated with different concentrations of chemically treated natural bone powder (NBP) (5, 10 and 15 wt%) to be used in the treatment of orthopedics bone diseases and fractures was prepared. Three different monomers, namely N-vinyl pyrrolidone (NVP), methyl methacrylate (MMA) and a mixture of NVP and MMA (1:1 by weight ratio) was used as crosslinking agent each separately. The composite samples were immersed in the simulated body fluid (SBF) for 30 days and studied through Fourier transform infrared (FTIR), scanning electron microscope (SEM), energy dispersive X-ray (EDX) in addition to dielectric measurements. The degradation time and the change in the pH of the SBF during the period of immersion were studied. From the FTIR, the increase intensity of absorption bands observed at 1076 cm^{-1} , 843 cm^{-1} , 711 cm^{-1} , and 578 cm^{-1} after immersion in SBF can be considered as good evidence for the formation of calcium phosphate layer which was also confirmed with the SEM and EDX tools. The dielectric measurements carried out on these prepared composites at frequency range from 100 Hz–100 kHz indicate that the permittivity ϵ' and dielectric loss ϵ'' follow the order $\text{NVP} > \text{NVP/MMA} > \text{MMA}$. Both parameters were found to increase by increasing the percentage of natural bone powder. The relaxation times obtained could be attributed, respectively, to Maxwell-Wagner effect and to the relaxation process related to carboxyl, hydroxyl, and ester functions associated with the main chain.

Keywords: Poly (propylene fumarate), calcium sulfate dihydrate, bone powder, composites, crosslinking agent, biodegradable, biophysical properties.

INTRODUCTION

Many researchers had focused on the biological and mechanical compatibility of the biomaterials ignoring that the smart biomaterial must be biologically, mechanically and electrically compatible.

Received: April 2015;
in final form May 2015.

There is tremendous amount of efforts to find the best potential bone graft substitutes including demineralized bone matrix or bone derivatives as bone morphogenic protein (BMP), osteogenin to be used, and synthetic graft materials lack osteoinductive or osteogenic elemental properties to the host [18].

Calcium sulfate dihydrate (gypsum) is a highly biocompatible material that has the characteristic of being one of the simplest synthetic graft materials. Moreover, crystallized calcium sulphate dihydrate was considered to be osteogenic *in vivo*. However, calcium sulfate cements might have few points of concerns: they undergo rapid passive dissolution even before the host bone has had time to grow into the defect area and pure calcium sulfate does not have the property of osteoconductivity [10].

Zamanian *et al.* [24] reported that replacement of nano hydroxyl apatite for calcium sulfate hemihydrate in powder phase of calcium sulfate cement greatly decreased the mechanical strength and increased setting time. However, better cell viability was experienced for fibroblasts at the presence of nanoapatite/calcium sulfate nanocomposite predicting its better biocompatibility in comparison to pure calcium sulfate. The setting time of nanocomposite is still suitable for surgical operation, the cement may be used for non-load bearing applications because of the reduced compressive strength.

Cai *et al.* [3] investigated the effects of PPF molecular weight and CaSO_4/TCP molar ratio on the *in vivo* degradation of poly (propylene fumarate) (calcium sulfate/tricalcium phosphate) (PPF/ $(\text{CaSO}_4/\text{TCP})$) composite, and the bone tissue response to PPF/ $(\text{CaSO}_4/\text{TCP})$. They concluded that no inflammatory reaction was observed after implantation, and the composites are capable of in situ pore forming. The pore forming rate can be adjusted by varying the composition of the composites.

Cross-linked Polypropylene fumarate (PPF) filled with different concentrations of Calcium sulfate dihydrate (gypsum) have been studied in our previous work [12]. The dielectric data as well as the mechanical ones indicate that 60% gypsum was characterized by the optimum properties. There was a rationale to reinforce the composite with rigid filler.

At the structural level the bones are composed of organic, inorganic compounds and water, being actually a composite material, each component contributing to the remarkable properties of bone. The organic part consists mainly in a network of collagen and proteins, while the inorganic component is mainly hydroxyapatite (HA), and a small percentage of other elements incorporated into the structure, such as magnesium and sodium carbonate [15, 23]. Researchers have highlighted the effect of the organic matrix on the mechanical properties of the whole biocomposites [4, 20]. A variety of methods have been used to produce powders from bone [11].

The aim of the present work is to study the effect of incorporation of different concentrations of natural bone powder (5, 10 and 15 wt%) on the biophysical

properties of polypropylene fumarate and calcium sulfate dehydrate (gypsum) composites cross-linked with N-vinyl pyrrolidone, methylmethacrylate and a mixture of them (1:1 wt%) to be used for bone regeneration. The apatite layer which is expected to be formed onto the surface of the samples by immersion in simulated body fluid (SBF) studied through the dielectric measurements, Fourier transform infrared (FTIR), scanning electron microscope (SEM), Energy dispersive X-ray (EDX). The biodegradation rate and the change in pH during immersion in simulated body fluid (SBF) are also studied.

MATERIALS AND METHODS

MATERIALS

Diethyl fumarate, 1,2-propanediol, and tetrabutyltitanate as the transesterification catalyst were reagent grade from Merck, Darmstadt, Germany, and used as received. N-vinyl pyrrolidone (NVP; freshly distilled) or methyl methacrylate (MMA; freshly distilled) were obtained from Merck, Darmstadt, Germany. Benzoyl peroxide, N, N-dimethyl-4-toluidine and gypsum [calcium sulfate dihydrate ($\text{CaSO}_4 \cdot 2\text{H}_2\text{O}$)] were obtained from Aldrich.

Polypropylene fumarate (PPF) was prepared by the two-stage melt polycondensation method (esterification and polycondensation) of (1 mol) diethyl fumarate and (2.2 mol) 1,2-propanediol in the presence of catalyst. The preparation and characterization of PPF were reported in details by the same authors [12].

Fumarate polyester resin (PPF) was cross-linked with 30% by weight of each of (N-vinyl pyrrolidone (NVP) or methylmethacrylate (MMA) or a mixture of (NVP/MMA) in the ratio of 1:1 by weight using benzoyl peroxide as initiator (2 wt%). N,N-dimethyl-4-toluidine (0.2 wt%) was added with rapid stirring, then the mixture was molded using appropriate molds for different tests. Curing occurred after leaving the mixtures at room temperature (25 °C) for 24 h.

The bone powder was prepared from freshly removed diaphyses of the calf long bones. Bones were dissected from the surrounding connective tissues then alkali treated to leave purely osseous structure free of all traces of tissues, fat or any organic matter occupying the intraosseous spaces. In alkali treatment, the bones were broken into small pieces and boiled for hours in a 30% sodium carbonate solution followed by thorough washing with hot water. The treated bones were then dried at 100 °C overnight. The cycle of alkali treatment was currently repeated till constant weight was reached. Then bones were ground to fine powders in a hardened steel vial. The bone powder was sieved to obtain the suitable particle size [17].

The composites were prepared by mixing 60 wt% gyp containing different concentrations of natural bone powder (5, 10 and 15 wt%) with a mixture of fumarate polyester resin (PPF) and each crosslinking agents namely NVP, MMA, and mix of NVP/MMA in the ratio of 1:1 by weight. All the samples were left for 24 h at 25 °C for curing.

To assess *in vitro* bioactivity, the composites were soaked in simulated body fluid (SBF) at 37 °C for 30 days, after which they were rinsed gently with deionized water and dried.

The disks were accurately weighed before and after immersion in SBF. The weight loss (WL) was calculated according to:

$$\text{Weight loss\%} = \frac{(W_0 - W_d)}{W_d} \times 100 \quad (1)$$

where W_0 is the initial weight of the specimen and W_d the weight of the specimen dried after different degradation times (7, 14, 21 and 28 days). All the measurements were taken in triplicate and the average values were calculated.

The pH value was measured during soaking in SBF and readings were taken in an mPA-210 pH meter at 37 °C.

CHARACTERIZATION TECHNIQUES

Transmission electron microscope (TEM) used to determine the particle size of the fillers was determined using transmission electron microscope model: Tecnai G 20, super twin, double tilt and magnification range up to 1,000,000 xs and applied voltage 200 kV. Gun type: LaB6 Gun Japan.

Scanning electron microscope coupled with energy dispersive X-ray (SEM/EDX, Philips XL30) Japan was used to study the morphology of the composite before and after soaking in SBF.

Fourier transform infrared (FTIR) was used to record the infrared spectrum by using JASCO FT/IR 300 E (Tokyo, Japan).

Dielectric measurements were carried out in the frequency range 100 Hz up to 100 kHz using (Ando Electric, Japan). The capacitance C , loss tangent $\tan \delta$, and ac resistance R_{ac} were measured directly from the bridge from which the permittivity ϵ' , dielectric loss ϵ'' and R_{dc} were determined. A guard ring capacitor type NFM/5T Wiss Tech. Werkstätten (WTW) GMBH Germany was used as a measuring cell. The cell was calibrated using standard materials and the experimental errors in ϵ' and ϵ'' were found to be $\pm 3\%$ and $\pm 5\%$, respectively. The temperature was controlled to 30 °C by using digital oven and the experimental error in the temperature was ± 0.1 °C.

RESULTS AND DISCUSSION

TRANSMISSION ELECTRON MICROSCOPE (TEM)

Microstructure of pure gypsum (Fig. 1) was found to consist of many sphere-like crystals entangled to each other with particle size in the range 50–91 nm.

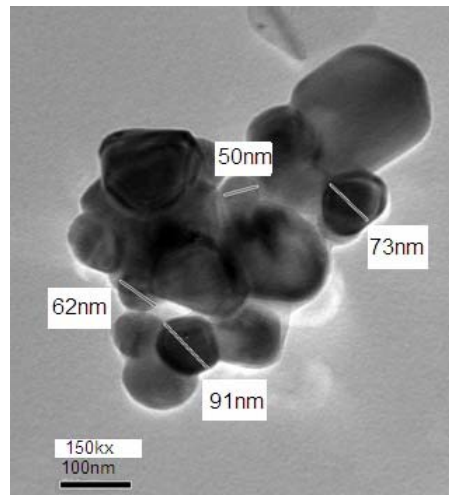


Fig. 1. TEM micrograph for gypsum.

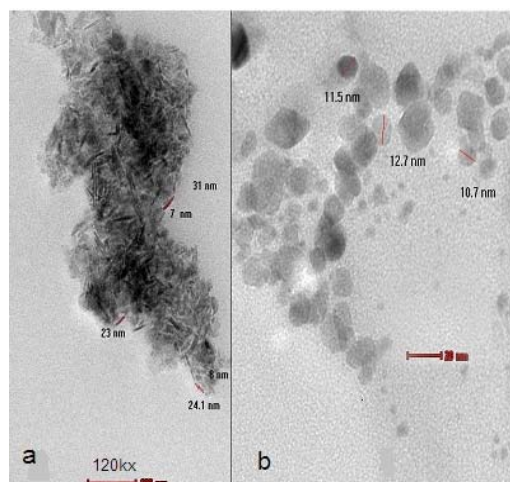


Fig. 2. TEM micrographs of (a) needle-like crystallites of HA (b) plate-like crystallites of the ground natural bone powder particles.

TEM for ground bone powder in (Fig. 2) reveals the presence of 2 families of particles, needle-like crystallites of HA (Fig. 2a) with needle length lie between 7 and 31 nm and second other family of plate-like apatite crystallites (Fig. 2b) of about 10–12 nm. TEM studies of animal bones have revealed that regularly arranged hydroxyapatite crystals occur within the collagen matrix in natural bones [14].

FOURIER TRANSFORM INFRARED (FTIR)

In order to analyze the chemical structure of the composites, the FTIR spectra are recorded in the spectral region 4000–400 cm^{-1} before and after immersion in the SBF. Figure 3 represents the FTIR spectrum of PPF/gyp composites cross-linked with NVP/MMA loaded with different concentrations of natural bone powder (5, 10 and 15 wt%) before immersion in SBF.

The spectra are gathering all the characteristic bands for the polymer, the gypsum and some minor bands characteristic for the included bone powder. The band assignments for PPF/gyp composites filled with 5 wt% NBP before immersion are given in Table 1.

FTIR spectra of composites before immersion are given in Table 1 and illustrated graphically in Figure 3. The figure shows vibration bands at 3530, 3408 cm^{-1} assigned to the molecular water. Intense strong band at 1740 cm^{-1} is characteristic to the stretching frequency of acid and ester carbonyl group of the PPF polymer. The band at 2960 cm^{-1} is due to stretching frequency of CH_2 . The presence of unsaturation $\text{C}=\text{C}$ in fumarate unit appears at 1678 cm^{-1} . The vibration bands at 660, 590 and 450 cm^{-1} along with strong doublet at 1142 cm^{-1} and 1122 cm^{-1} are due to sulfate group SO_4^{-2} of the calcium sulphate dihydrate.

The peaks of residual organic matter of natural bone powder appears at 2960, 1684 and 1590 cm^{-1} [17]. The shoulder observed at 760 cm^{-1} and 870 cm^{-1} in addition to minor bands at 1415 cm^{-1} and 1447 cm^{-1} correspond to vibrational mode of carbonate group due to the presence of natural bone powder. By increasing the concentrations of NBP, in Figure 3 the peaks of residual organic matter (2960, 1684 and 1590 cm^{-1}) along with the peaks of the inorganic part of natural bone (hydroxyapatite phosphate group) at 602 and 570 cm^{-1} exhibit higher intensity.

After 30 days of immersion, the outer layers of these samples were peeled off and studied by FTIR spectroscopy and illustrated in Figure 4.

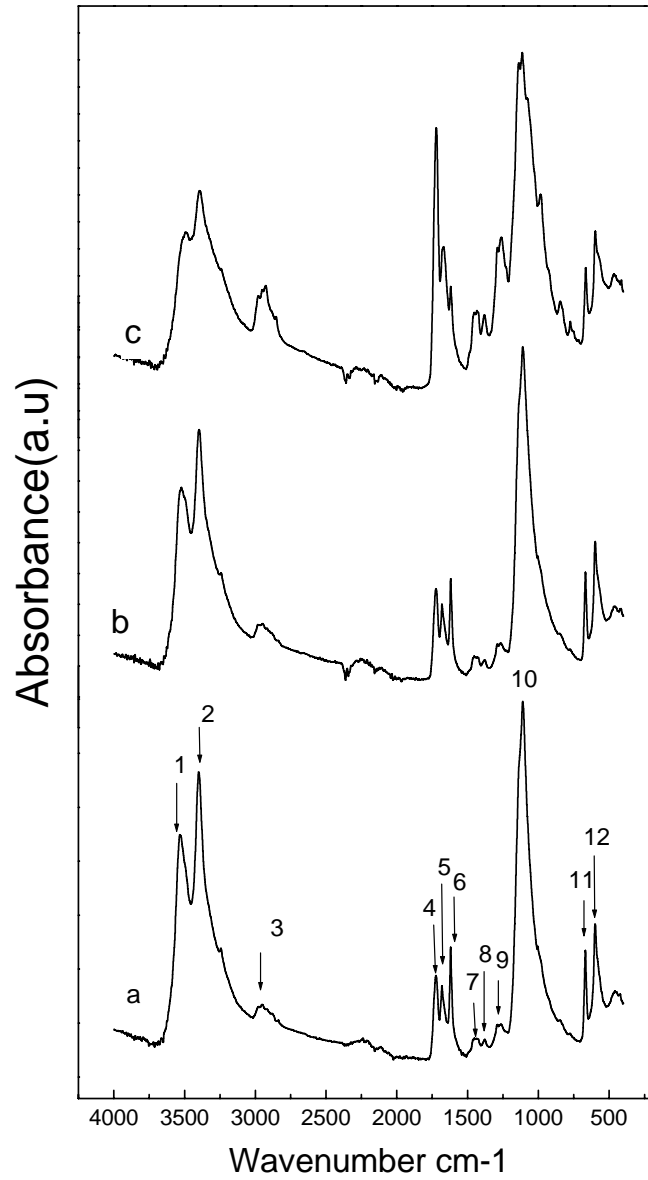


Fig. 3. FTIR spectrum of PPF/gyp composites cross-linked with NVP/MMA, loaded with (a) 5 wt%, (b) 10 wt% and (c) 15 wt% NBP before immersion in SBF.

Comparing the spectra of the PPF/gyp composite filled with 5 wt% NBP before and after immersion, Figure 4, there is no evidence for the presence of gypsum after immersion since the specific two absorption bands at 665 cm^{-1} and 604 cm^{-1} due to OS–O bending vibrations disappeared.

Decreasing in the intensity of the strong doublet at 1142 cm^{-1} and 1122 cm^{-1} due to sulfate group is observed. New bands appear at 752 cm^{-1} , 863 cm^{-1} and 987 cm^{-1} attributed to the carbonate group [19]. The new band at 1052 cm^{-1} is characteristic for the phosphate group. The bands at 1415 cm^{-1} due to C–O stretch and 1444 cm^{-1} correspond to vibrational mode of carbonate group exhibited increasing in the intensities. A similar trend was observed for all the investigated composites. Therefore, the IR results can indicate the converting of calcium sulphate to calcium phosphate and that the carbonated apatite is deposited on the outer layer of the prepared sample as a result of immersion in the SBF for 30 days.

Table 1

FTIR band assignments for PPF/gyp/NBP composites cross-linked with NVP/MMA before immersion in SBF

Bands no.	Bands (cm^{-1})	Assignments
1	3530	stretching mode of hydrogen-bonded OH^- ions
2	3408	OH groups
3	2960	Stretching frequency of CH_2
4	1740	stretching frequency of acid and estercarbonyl group
5	1678	Unsaturation $\text{C}=\text{C}$ in fumarate unit
6	1617	$\text{C}=\text{O}$ stretching of amide I
7	1447	vibrational mode of carbonate group
8	1415	
9	1280	C–O stretch
10	1122 1142	Sulfate group
11	660	OS–O bending vibrations
12	604	

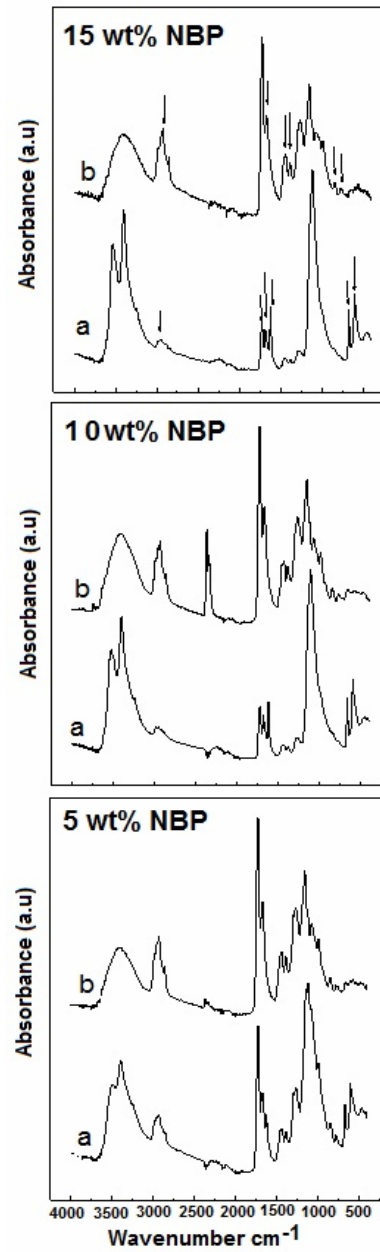


Fig. 4. FTIR spectra of PPF/gyp composites cross-linked with NVP/MMA loaded with different concentrations of NBP (a) before and (b) after immersion in SBF for 30 days.

SCANNING ELECTRON MICROSCOPE (SEM)
AND ENERGY DISPERSIVE X-RAY (EDX) ANALYSIS

Standard *in vitro* bioactivity test was carried out to evaluate the formation of an apatite layer onto the surface of the composites. The surface morphology of the cross-linked PPF/gyp composites loaded with different concentrations of bone powder was examined by scanning electron microscope (SEM) and the elemental analysis carried out by the energy dispersive X-ray (EDX) technique before and after 30 days of immersion in SBF. The results are illustrated in Figures 5–7 for composites cross-linked with NVP/MMA as an example. Comparing the SEM images before and after immersion, it is clear that before immersion, composites show smooth surfaces which revealed a homogeneous distribution of the filler particles within the polymer matrix. After immersing the specimens 30 days in the SBF solution, the structure showed pores and cavities which were attributed to their ability to undergo hydrolysis. The presence of small and large spherical particles with bright white color denotes the formation of calcium phosphate particles onto the surfaces.

The EDX patterns before immersion show the presence of carbon (C) and oxygen (O₂) originating from the PPF polymer structure, calcium (Ca) and sulfur (S) as main elements of the incorporated gypsum. Weak signals of phosphorous (P), sodium (Na), magnesium (Mg) as a result of incorporation of the bone powder are noticed [15]. After immersion, the EDX spectra reveal a remarkable increase in the signals of phosphorus (P) and the depletion of sulfur (S) which emphasize that the calcium sulphates replaced by calcium phosphate due to the reaction with SBF solution. The nature of the calcium phosphate layer formed on the surface of the samples is detected from the calculated phosphocalcic ratios.

The Ca–P ratios of the samples after immersion for 30 days in SBF are 1.52, 1.64 and 1.89 for PPF/gyp composites cross-linked with MMA and loaded with 5, 10 and 15 wt% NBP respectively.

The Ca–P ratios of the samples after immersion for 30 days in SBF are 2.1, 2.5 and 3 for PPF/gyp composites cross-linked with NVP and loaded with 5, 10 and 15 wt% NBP respectively.

The Ca–P ratios of the samples after immersion for 30 days in SBF are 2.03, 2.2 and 3 for PPF/gyp composites cross-linked with NVP/MMA and loaded with 5, 10 and 15 wt% NBP respectively.

For the PPF/gyp composites cross-linked with MMA, the ratios of the Ca–P are close to the stoichiometric biological apatite (1.67) [5, 22]. The increased phosphocalcic ratio for NVP and NVP/MMA cross-linked samples may be attributed to the presence of negatively charged carboxylate group of N-vinyl pyrrolidone which may attract calcium ions present in the SBF solution and favor calcium phosphate apatite nucleation [7]. The composites cross-linked with NVP and NVP/MMA loaded with 15 wt% NBP, the CA–P ratio reached 3. This increase in the calcium content with respect to phosphorus may reflect some decrease in the apatite formation so the surface is not fully covered with apatite and the X-ray beam could detect the calcium in the matrix.

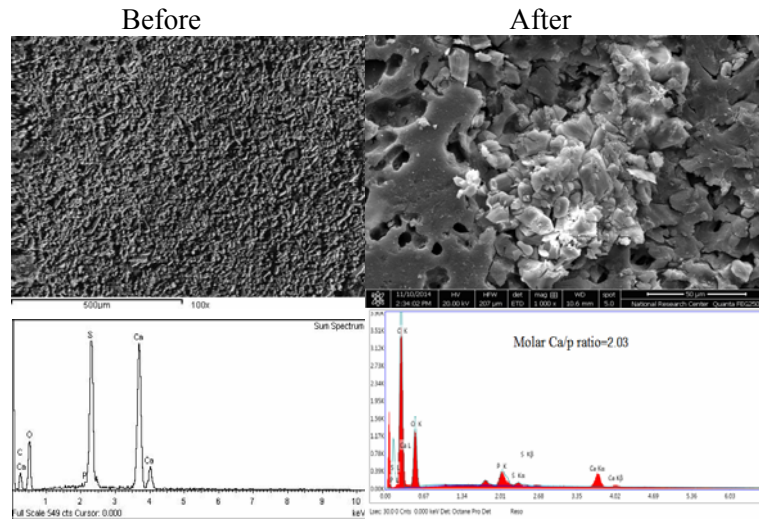


Fig. 5. SEM micrograph and EDX spectrum of PPF/gyp composites cross-linked with NVP/MMA and filled with 5 wt% NBP before and after immersion in SBF for 30 days.

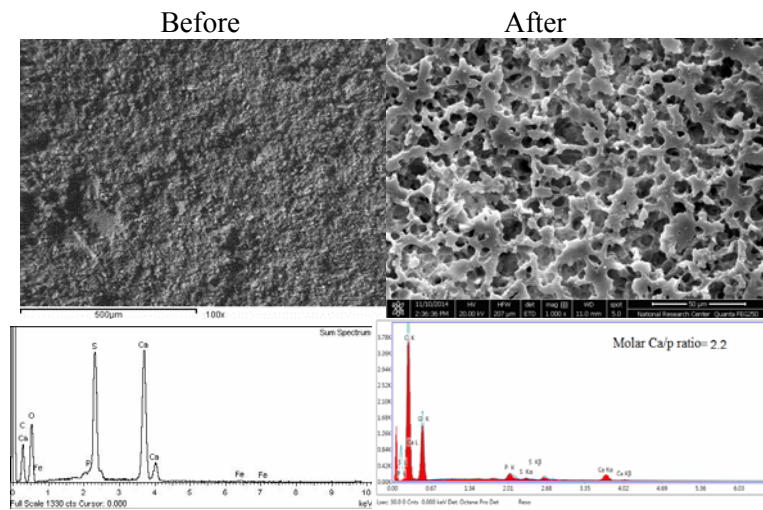


Fig. 6. SEM micrograph and EDX spectrum of PPF/gyp composites cross-linked with NVP/MMA and filled with 10 wt% NBP before and after immersion in SBF for 30 days.

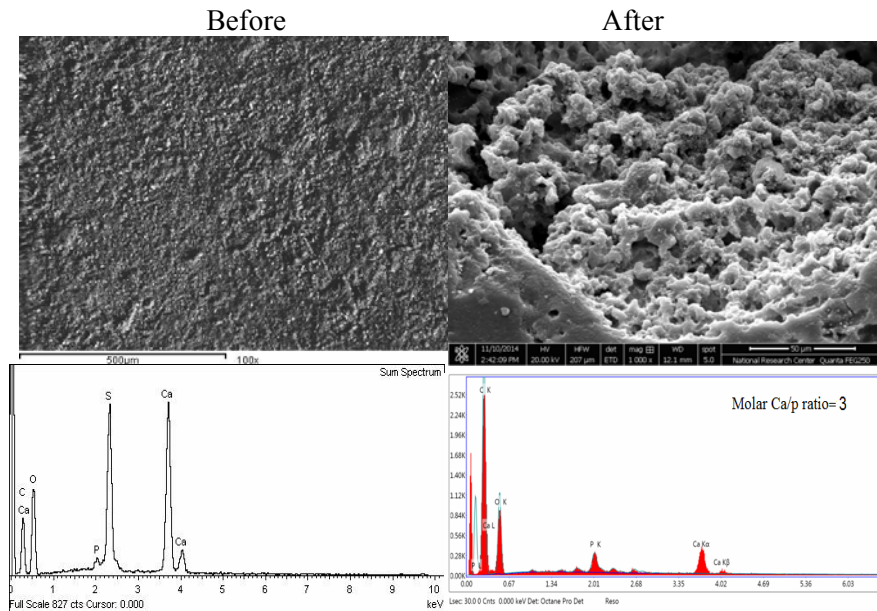


Fig. 7. SEM micrograph and EDX spectrum of PPF/gyp composites cross-linked with NVP/MMA and filled with 15 wt% NBP before and after immersion in SBF for 30 days.

DEGRADATION RATE

The limitation of using calcium sulphates in cement composites is that they undergo rapid passive dissolution and exhibit high rates of *in vivo* resorption even before the host bone had had time to grow into the defect area [10].

The rate of degradation of the composites reinforced with bone powder was significantly slower compared with those of PPF/gyp composites [12]. The high content of bone morphogenetic proteins resulted in high degree of stability in SBF [7]. The natural bone powder content had great effect on the stability of the composites during the degradation. Figure 8 shows the degradation rate for PPF/gyp/NBP composites after different soaking times. From this figure it is observed that, by increasing the concentration of bone powder there was a decrease in the degradation rate, *i.e.* decreasing the weight loss for all the composites. Also it is worth mentioning that the degradation of PPF cross-linked with NVP is slower than that of MMA and NVP/MMA.

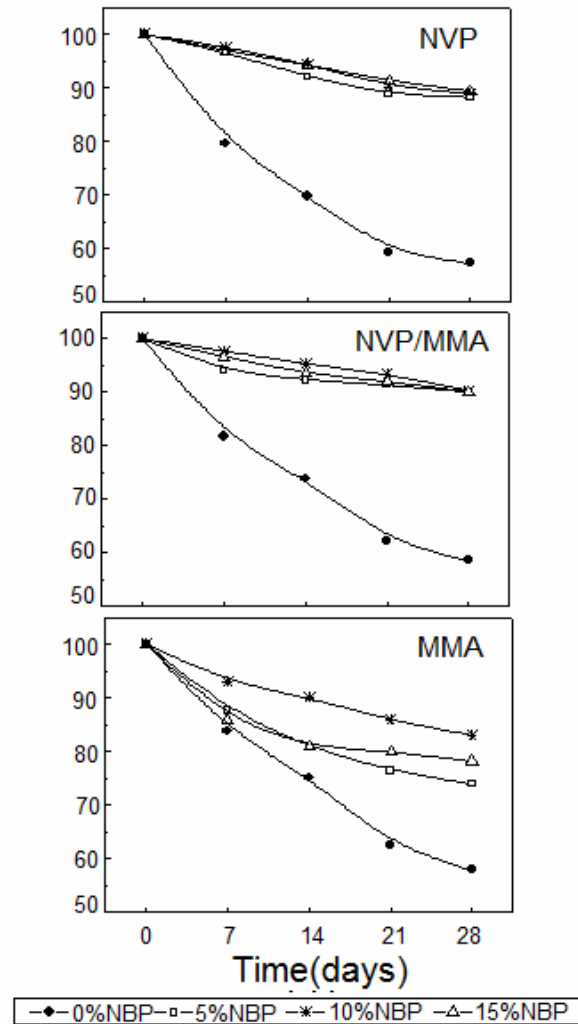


Fig. 8. The degradation rate for PPF/gyp/NBP composites after different soaking times.

pH MEASUREMENTS

The pH of the SBF solution during immersion of the samples was measured to monitor the changes that could be a combination of acidic degradation by-products resulting from the polymer and any neutralization effects resulting from the fillers.

For all samples there was a rapid change in the pH of the SBF at the first 3 days of immersion as a result of dissolution of the composites which suggests high reactivity of these composites. The decrease in the pH values reached a lowest value ranging from 4.5–5 for PPF/ gyp/NBP composites.

DIELECTRIC MEASUREMENTS

Dielectric spectroscopy measurements achieve a new contribution for understanding the dynamics of the formation of apatite structure through the relaxation phenomenon corresponding to the terminal polar groups, carboxyl and hydroxyl functions, and to ester functions in the polymer chain [6]. For such reason the aim of this part of work is to employ such tool to follow the expected formation of such a structure which was expected to take place by immersing the investigated samples in the SBF.

The frequency dependence of the permittivity ϵ' and dielectric loss ϵ'' over the frequency range from 100 Hz–100 kHz and at 30 °C for poly (propylene fumarate) (PPF/gyp), cross-linked with different crosslinking agents MMA, NVP/MMA and NVP and loaded with different concentrations (5, 10 and 15 wt%) of natural bone powder (NBP), is presented in Figures 9–11. The data of ϵ' given for such composites are comparable with that found in case of natural bone [13]. From these figures, it is seen that both ϵ' and ϵ'' increase by increasing the filler content. Also, ϵ' for the whole investigated samples decreases with increasing the frequency, which shows anomalous dispersion.

On the other hand, the absorption curves of ϵ'' *versus* the frequency f shown in Figures 9–11 are broad indicating that more than one relaxation mechanism is present. It is also clear that the values of ϵ' and ϵ'' increase in the order MMA < NVP/MMA < NVP. This may be due to the higher polarity of NVP (4D) [9] compared with that of MMA (1.79 D) [2].

In addition to the conductivity term, the analysis of the absorption curves relating ϵ'' and the applied frequency after subtracting the conductivity term was done in terms of superposition of one Fröhlich and Havriliak-Negami functions [9]. The absorption region detected at lower frequency range is fitted by Fröhlich function with distribution parameter $p = 3$ and relaxation time τ_1 ranging from to 3.5 to 3.8×10^{-10} s. The relaxation time associated with such a process is found to be independent of the type of the monomer used for crosslinking. This absorption region could be attributed to Maxwell-Wagner effect [12]. As it is expected it is to be found at the lower frequency range due to the multi constituent of the investigated systems.

The second absorption region τ_2 in the higher frequency range could be fitted by Havriliak-Negami function with distribution parameters $\alpha = 0.5$ and $\beta = 0.5$ according to the equation given elsewhere [1] that could be ascribed with some local molecular motions rather than the main chain motion. The relaxation time τ_2 and the relaxation strength S_2 obtained for such region together with the electrical conductivity σ are given in Table 2. This relaxation corresponds to the terminal polar groups, carboxyl and hydroxyl functions, and to ester functions in the polymer chain. The relaxation time associated with this region is found to be highly affected by the type of crosslinking agent and follows the order MMA > NVP/MMA > NVP, i.e., depending on the molar volume of the rotating units and consequently on the relaxation time.

From Table 2 it is notable that by increasing the filler content the values of the relaxation time τ_2 , the relaxation strength S_2 and the electrical conductivity σ are also increased.

After immersing the cross-linked composites in SBF solution for 30 days, the permittivity ϵ' and dielectric loss ϵ'' were re-measured. Comparing the data obtained before and after immersing in SBF Figures 9–11, it is seen that both ϵ' and ϵ'' decrease by immersing in the SBF solution. This decrease could be attributed to the formation of apatite structure that takes some ions to crystal formation where they are no longer mobile and no longer contributed to the dielectric spectrum [16]. The curves relating ϵ'' and the applied frequency were analyzed and the obtained data are given in Table 3.

Comparing Tables 2 and 3 it is interesting to find that both conductivity and S_2 decrease, whereas a pronouncing increase in τ_2 is noticed. The increase in τ_2 reflects an increase in the molar volume of the rotating units due to the formation of apatite structure that takes some ions to crystal formation to become no longer mobile and thus no longer contributing to the dielectric spectrum. To find an expression to distinguish between the amounts of apatite structure which is expected to be formed by immersing the investigated samples in SBF, the relation $(\tau_{\text{aft}} - \tau_{\text{bef}}) / \tau_{\text{bef}}$ was calculated and listed in Table 3. From this table, it is interesting to notice that the values of $(\tau_{\text{aft}} - \tau_{\text{bef}}) / \tau_{\text{bef}}$ increase according to the NVP > NVP/MMA > MMA. The enhancement of apatite formation by the addition of natural bone powder is attributed to the presence of osteo-inductive substances such as growth factors (IGF, FGF, PDGF, etc.) and bone morphogenetic proteins (BMPs). These proteins stimulate bone regeneration by inducing stem cell differentiation to bone forming cells (osteoblasts) [8].

These results could recommend NVP/MMA to be used in crosslinking polypropylene fumarate rather than the expensive monomer NVP and the unrecompensed one MMA. In addition, from Table 3 it is noticed that the highest values for $(\tau_{\text{aft}} - \tau_{\text{bef}}) / \tau_{\text{bef}}$ are detected for composites containing 10% bone powder and the highest value was for that of NVP/MMA.

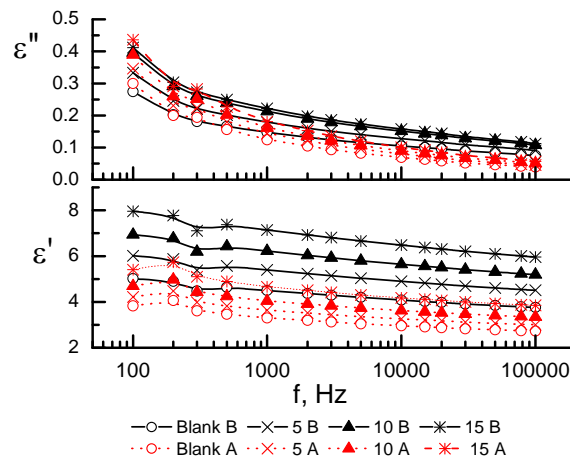


Fig. 9. Permittivity ϵ' and dielectric loss ϵ'' for PPF/gyp cross-linked with MMA and filled with different concentrations of NBP before (B) and after (A) immersing in SBF.

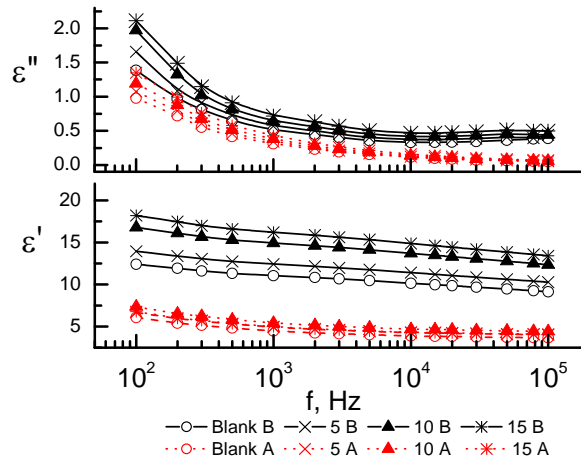


Fig. 10. Permittivity ϵ' and dielectric loss ϵ'' for PPF/gyp cross-linked with NVP and filled with different concentrations of NBP before (B) and after (A) immersing in SBF.

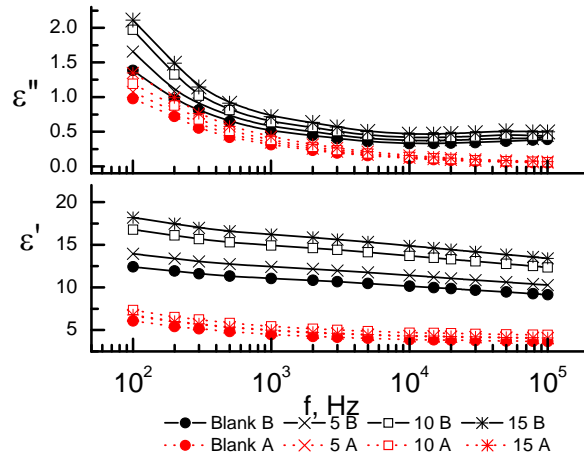


Fig. 11. Permittivity ϵ' and dielectric loss ϵ'' for PPF/gyp cross-linked with NVP/MMA and filled with different concentrations of NBP before (B) and after (A) immersing in SBF.

Table 2

Dielectric parameters of the composites under investigations

NBP (%)	$\sigma (\Omega^{-1} \text{ cm}^{-1} \times 10^{11})$	$\tau_2 \times 10^5 (\text{s})$	S_2
PPF/gyp cross-linked with NVP			
0	6.93	0.80	2.24
5	7.66	0.89	2.51
10	8.75	0.92	2.853
15	10.02	1.12	2.952
PPF/gyp cross-linked with NVP/MMA			
0	5.10	1.65	1.63
5	4.96	2.05	1.73
10	5.31	2.22	1.79
15	5.88	2.51	1.85
PPF/gyp cross-linked with MMA			
0	1.30	3.50	0.55
5	1.32	4.85	0.71
10	1.44	5.05	0.84
15	1.61	5.22	0.87

Table 3

Dielectric parameters of the composites under investigations after immersing in SBF for 30 days

NBP (%)	$\sigma (\Omega^{-1} \text{cm}^{-1} \times 10^{11})$	$\tau_2 \times 10^5 (\text{s})$	S_2	$(\tau_{\text{aft}} - \tau_{\text{bef}}) / \tau_{\text{bef}}$
PPF/gyp cross-linked with NVP				
0	4.49	3.51	0.50	3.39
5	4.54	4.55	0.415	4.11
10	5.3	5.2	0.727	4.65
15	6.1	5.5	0.791	4.02
PPF/gyp cross-linked with NVP/MMA				
0	3.70	6.39	0.63	2.87
5	4.8	8.00	1.70	2.9
10	5.12	8.81	1.88	3.0
15	5.31	9.5	2.01	2.8
PPF/gyp cross-linked with MMA				
0	1.12	10.20	0.35	1.91
5	1.35	15.02	0.44	2.096
10	1.6	17.12	0.50	2.39
15	1.82	17.8	0.54	2.41

CONCLUSION

The results could recommend the mixture of NVP/MMA to be used in crosslinking polypropylene fumarate rather than the expensive monomer NVP and the unrecompensed one MMA.

The addition of bone powder increases the stability of the composites during immersion in SBF.

The formation of calcium phosphate layer on the surface of composites after immersion in the simulated body fluid (SBF) was confirmed through: formation of white sphere crystals appeared on the SEM images, the change in the intensities of the bands noticed on FTIR charts and the pronounced increase in the relaxation time associated with the local molecular motions obtained from the analysis carried out on the absorption curves relating the dielectric loss ϵ'' versus frequency in terms of the superposition of Fröhlich and Havriliak-Negami functions.

Addition of natural bone powder favours the apatite formation. This attributes to the presence of osteo-inductive substances such as growth factors (IGF, FGF, PDGF, etc. and bone morphogenetic proteins (BMPs). These proteins stimulate bone regeneration by inducing stem cell differentiation to bone forming cells (osteoblasts).

10 wt% NBP is the optimal concentration to be used in such composites.

The composites are electrically compatible with natural bone.

REFERENCES

1. ABD-EL-MESSIEH, S.L., K.N. ABD - EL - NOUR, Effect of curing time and sulfur content on the dielectric relaxation of styrene butadiene rubber, *J. Appl. Polym. Sci.*, 2003, **88**, 1613–1621.
2. ABD-EL-MESSIEH, S.L., Dielectric relaxation of binary systems of some disubstituted fumarates with acrylonitrile and vinyl acetate in CCl₄ solutions, *J. Mol. Liq.*, 2002, **95**, 167–182.
3. CAI, Z., T. ZHANG, L. DI, D.M. XU, D.H. XU, D.A. YANG, Morphological and histological analysis on the *in vivo* degradation of poly (propylene fumarate) / (calcium sulfate/ β -tricalcium phosphate), *Biomedical Microdevices*, 2011, **13**(4), 623–631.
4. FANTNER, G.E., H. BIRKEDAL, J.H. KINDT, T. HASSENKAM, J.C. WEAVER, J.A. CUTRONI, B.L. BOSMA, L. BAWAZER, M.M. FINCH, G.A. CIDADE, D.E. MORSE, G.D. STUCKY, P.K. HANSMA, Influence of the degradation of the organic matrix on the microscopic fracture behavior of trabecular bone, *Bone*, 2004, **35**, 1013–1022.
5. FATHI, M.H., A. HANIFI, V. MORTAZAVI, Preparation and bioactivity evaluation of bone-like hydroxyapatite nanopowder, *Journal of Materials Processing Technology*, 2008, **202**, 536–542.
6. FISHER, J.P., T.A. HOLLAND, D. DEAN, P.S. ENGEL, A.G. MIKOS, Synthesis and properties of photocross-linked poly (propylene fumarate) scaffolds, *J. Biomater. Sci. Polym. Ed.*, 2001, **12**, 673–687.
7. HAROUN, A.A., V. MIGONNEY, Synthesis and *in vitro* evaluation of gelatin/hydroxyapatite graft copolymers to form bionanocomposites, *International Journal of Biological Macromolecules*, 2010, **46**, 310–316.
8. HOROWITZ, R.A., Z. MAZOR, C. FOITZIK, H. PRASAD, M. ROHRER, A. PALTI, β -tricalcium phosphate as bone substitute material: properties and clinical applications, *Titanium*, 2009, **1**(2), 1–11.
9. HU, Y., H.R. MOTZER, A.M. ETXEBERRIA, M.J. FERNANDEZ-BERRIDI, J.J. IRUIN, P.C. PAINTER, M.M. COLEMAN, Concerning the self-association of N-vinyl pyrrolidone and its effect on the determination of equilibrium constants and the thermodynamics of mixing, *Macromol. Chem. Phys.*, 2000, **201**, 705–714.
10. JALOTA, S., B. SARIT, A. BHADURI, T. CUNEYT, Using a synthetic body fluid (SBF) solution of 27 mM HCO₃⁻ to make bone substitutes more osteo-integrative, *Materials Science and Engineering C*, 2008, **28**(1), 129–140.
11. JOHNSON, G.S., M.R. MUCALO, M.A. LORIER, U. GIELAND, H. MUCHA, The processing and characterization of animal-derived bone to yield materials with biomedical applications. Part II: milled bone powders, reprecipitated hydroxyapatite and the potential uses of these materials, *J. Mat. Sci.: Mat. Med.*, 2000, **11**, 725–741.
12. KAMEL, N.A., T.H. ABOU-AIAAD, B.A. ISKANDER, S.K.H. KHALIL, S.H. MANSOUR, S.L. ABD-EL-MESSIEH, K.N. ABD-EL-NOUR, Biophysical studies on bone cement composites based on polyester fumarate, *J. Appl. Polym. Sci.*, 2009, **116**(2), 876–885.
13. MARZEC, E., A comparison of dielectric relaxation of bone and keratin, *Bioelectrochemistry and Bioenergetics*, 1998, **46**, 29–32.
14. MASAKUNI, O., S. SUGURU, microstructural development of natural hydroxyapatite originated from fish-bone waste through heat treatment, *J. Am. Ceram. Soc.*, 2002, **85**(5), 1315–1317.
15. MICULESCU, F., L.T. CIOCAN, M. MICULESCU, A. ERNUTEANU, Effect of heating process on micro structure level of cortical bone prepared for compositional analysis, *Digest Journal of Nanomaterials and Biostructures*, 2011, **6**(1), 225 – 233.
16. MOHAMED, M.G., S.L. ABD-EL-MESSIEH, S. EL-SABBAGH, A.F. YOUNAN, Electrical and mechanical properties of polyethylene-rubber blends, *J. Appl. Polym. Sci.*, 1998, **69**, 775.

17. MOHARRAM, M.A., M.A. ALLAM, Study of the interaction of poly (acrylic acid) and poly (acrylic acid-poly acrylamide) complex with bone powders and hydroxyapatite by using TGA and DSC, *Journal of Applied Polymer Science*, 2007, **105**(6), 3220–3227.
18. OGURTAN, Z., F. HATIPOGLU, C. CEYLAN, Comparative evaluation of demineralized and mineralized xenogeneic bovine bone powder and chips on the healing of circumscribed radial bone defects in the dog, *Araştırma*, 2007, **21**(6), 269 – 276.
19. PASCHALIS, E.P., E. DICARLO, F.BETTS, R. MENDELSON, A.L. BOSKEY, FTIR micro spectroscopic analysis of normal human cortical and trabecular bone, *Calcified Tissue International*, 1997, **61**, 480–486.
20. ROSEN, V.B., L.W. HOBBS, M. SPECTOR, The ultrastructure of an organic bovine bone and selected synthetic hydroxyapatites used as bone graft substitute materials, *Biomaterials*, 2002, **23**, 921–928.
21. ROZIK, N.N., S.L. ABD-EL MESSIEH, A.A. YASEEN, A.A. SHOUK, Dielectric and mechanical properties of natural nanofibers-reinforced ethylene propylene diene rubber: carrot foliage and corn gluten, *Polymer Engineering And Science*, 2013, **53**(4), 874–881.
22. SAKAE, T., H. NAKADA, Historical review of biological apatite crystallography, *Journal of Hard Tissue Biology*, 2015, **24**(2), 111–122.
23. YANG, H., X. YAN, M. LING, Z. XIONG, C. OU, W. LU, *In vitro* corrosion and cytocompatibility properties of nano-whisker hydroxyapatite coating on magnesium alloy for bone tissue engineering applications, *International Journal of Molecular Sciences*, 2015, **16**(3), 6113–6123.
24. ZAMANIAN, A., S. HESARAKI, M. KHORAMI, Physical and *in vitro* biological evaluation of a novel calcium sulfate-apatite nanocomposite, *Journal of the Australian Ceramic Society*, 2010, **46**(2), 43–47.